Using wavelets to solve the Burgers equation: A comparative study

R. L. Schult and H. W. Wyld

Department of Physics, University of Illinois at Urbana-Champaign, 1110 West Green Street, Urbana, Illinois 61801

(Received 26 June 1992)

The Burgers equation is solved for Reynolds numbers $\lesssim 8000$ in a representation using coarse-scale scaling functions and a subset of the wavelets at finer scales of resolution. Situations are studied in which the solution develops a shocklike discontinuity. Extra wavelets are kept for several levels of higher resolution in the neighborhood of this discontinuity. Algorithms are presented for the calculation of matrix elements of first- and second-derivative operators and a useful product operation in this truncated wavelet basis. The time evolution of the system is followed using an implicit time-stepping computer code. An adaptive algorithm is presented which allows the code to follow a moving shock front in a system with periodic boundary conditions.

PACS number(s): 03.40.Kf, 02.60.+y, 02.50.+s, 02.70.+d

I. INTRODUCTION

The nonlinear partial differential equations which describe physical phenomena, e.g., the equations of fluid mechanics, are usually not susceptible to analytic solution. Several options are available for numerical solution. The simplest is straightforward finite differencing on a uniformly spaced grid of points. This is effective for one-dimensional systems, but the number of grid points needed grows rapidly with the number of dimensions. A three-dimensional system with 10^3 grid points is easy, with 100^3 is perhaps barely feasible on the computers of today, but with 1000^3 is not. If the phenomena of interest have linear scales less than $L/10$ or $L/100$, where L is the linear dimension of the system, straightforward uniform finite differencing may fail.

Another option is expansion in a basis of appropriately chosen modes. The most common choice is, of course, Fourier expansion. In order to reduce the number of modes needed, they should be chosen with an eye to the underlying physics. If the physics is well described by monochromatic waves, Fourier expansion would seem to be a good choice. An important feature of Fourier modes is their mutual orthogonality, which simplifies the details of the computation. Also, truncation of the mode expansion at a specified level means a certain well-defined sector of the underlying function space is being ignored. For truncated Fourier expansions small wavelengths are ignored.

Another important consideration is the ease or difficulty of expressing the operators of the theory in the chosen basis. Differential operators become multiplicative factors in a Fourier basis, so this aspect is very favorable for that choice of modes. Differential operators are more difficult in the finite-differencing scheme, but still have simplifying features: In the lowest-order schemes, derivatives introduce interactions between nearest neighbors. This leads to tridiagonal matrices in one-dimensional problems and matrices with a well-defined form of sparseness in higher dimensions.

Recently, the use of expansions in bases of orthogonal scaling functions and wavelets has become popular [1–5]. Each of the individual functions in such a basis is localized about a certain center and has a certain scale or width. The expansion is made in a series of functions of ever-decreasing scale localized about ever more closely spaced centers. Daubechies scaling functions and wavelets have compact support, while maintaining orthogonality. The most successful uses of these bases appear to be in data analysis and signal compression applications.

One might hope that the scaling function plus wavelet basis would be useful in the solution of nonlinear differential equations describing complicated phenomena leading to singularities or scaling behavior. Examples familiar from fluid mechanics are the discontinuities at shock waves and the "small vortices on bigger vortices" picture of turbulence. It might be possible to use the multiresolution properties [6] of scaling functions and wavelets advantageously in the turbulence problem. Preliminary work along these lines has been performed by Weiss [7]. For the shock-wave problem, one might use the localization properties by keeping more wavelets centered near the shock-wave discontinuity.

We have applied wavelets to the shock-wave-like phenomena which arise in the solution of the Burgers equation. Several papers have already appeared on this subject [8–11]. We follow the line of investigation pioneered by Tenenbaum and co-workers [8,10–12]. By using wavelets as well as scaling functions and by keeping a series of wavelets of smaller and smaller scale near the discontinuity we are able to avoid the Gibbs-like oscillations which plagued the solutions of these authors. We have also developed a primitive type of adaptive code which allows us to solve the Burgers equation for a situation with a moving shock front, as well as the fixed shock front considered by the above-mentioned authors.

Finally, we have attempted to compare three algorithms: (1) straightforward finite differencing with a uniform grid, (2) expansion in a basis of scaling functions as recommended by the Aware group, and (3) expansion in a basis of scaling functions and wavelets.

The Burgers equation, appropriate initial conditions, and the form of the solution are recalled in Sec. II. In Sec. III we discuss the calculation of the matrix elements of the necessary differential operators in our coarse-scale scaling function plus truncated wavelet basis. This is partly a review of parts of a more general calculation presented by Latto, Resnikoff, and Tenenbaum [12]. In Secs. IV and V we present our calculation using the combined scaling function wavelet basis with wavelets of fine scale near the discontinuity. This calculation is compared with a finite difference calculation and a calculation using only scaling functions.

II. THE BURGERS EQUATION

The simplest equation incorporating both nonlinear convection and diffusion is the Burgers equation,

$$\frac{\partial u}{\partial t}+u\frac{\partial u}{\partial x}=\nu\frac{\partial^2 u}{\partial x^2} . \tag{2.1}$$

It can be solved analytically with the aid of the Cole-Hopf transformation [13,14], which leads to a rather complicated formula that must be evaluated numerically.

Here we discuss direct numerical solution of the differential equation leading to the results presented in Figs. 1–3. We employ periodic boundary conditions in the region $0\leq x\leq L$. For Fig. 1 the initial condition was $u(x,0)=\sin(2\pi x/L)$, $0\leq x\leq L$. For Figs. 2 and 3 the initial condition had just the left half of the sine wave: $u(x,0)=\sin(2\pi x/L)$, $0\leq x\leq L/2$; $u(x,0)=0$, $L/2\leq x\leq L$. For both sets of initial conditions the sine curve steepens as time advances, eventually leading to a discontinuity. For the full sine wave, the discontinuity is stationary, while for the half-sine-wave initial condition, the discontinuity propagates to the right. Soon after the discontinuity develops the curves away from the discontinuity become straight lines, with slope gradually decreasing with time.

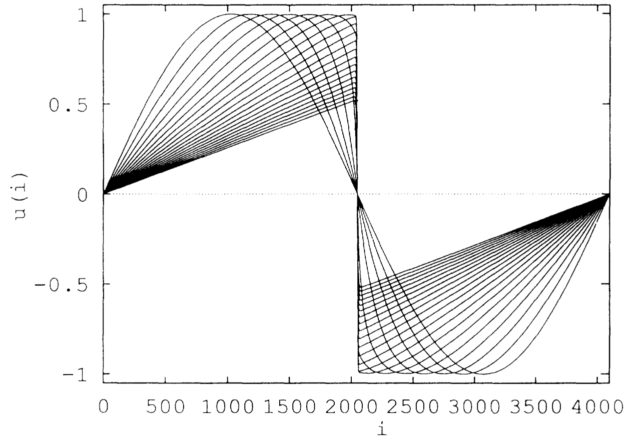

FIG. 1. Solution of the Burgers equation (2.1) at equally spaced time intervals for an initial condition $u(x,0)=\sin(2\pi x/L)$, $0\leq x\leq L$. The x interval is represented on a grid of 4096 points, $x/L=i/4096$, $i=1,4096$. As time advances the curves steepen, developing a shocklike discontinuity. The time interval between curves is 160 in grid units, i.e., $\Delta tu_{\max}/a=160$ with $a=L/4096$ and $u_{\max}=1$. The calculation was performed in a basis with 32 coarse-scale scaling functions and $7\times12=84$ wavelets at seven higher levels of resolution centered at the evolving discontinuity. In units of the grid spacing $\nu=2.048$, corresponding to a Reynolds number $4096/2.048=2000$.

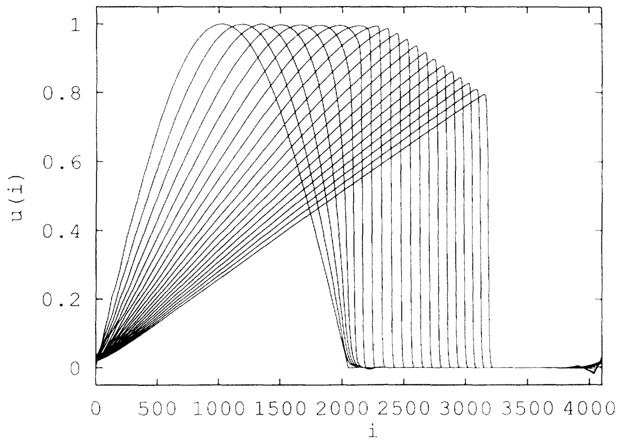

FIG. 2. Solution of the Burgers equation (2.1) at equally spaced time intervals for an initial condition $u(x,0)=\sin(2\pi x/L)$, $0\leq x\leq L/2$; $u(x,0)=0$, $L/2\leq x\leq L$. The x interval is represented on a grid of 4096 points, $x/L=i/4096$, $i=1,4096$. As time advances the curves steepen, developing a moving shocklike discontinuity. The time interval between curves is 160 in grid units, i.e., $\Delta tu_{\max}/a=160$ with $a=L/4096$ and $u_{\max}=1$. The calculation was performed in a basis with 32 coarse-scale scaling functions and $7\times12=84$ wavelets at seven higher levels of resolution centered at the evolving discontinuity. In units of the grid spacing $\nu=2.048$, corresponding to a Reynolds number $4096/2.048=2000$.

We can understand these features qualitatively without any elaborate calculations. It is clear from the differential equation that at positions x where u and $\partial u/\partial x$ have the same sign, u will decrease with time, and where they have opposite signs u will increase. This explains the steepening of the sine curve with time. After the curves have evolved to straight lines, it is easy to find the analytic solution

$$u=\frac{x}{t+d_0} , \tag{2.2}$$

where the integration constant $d_0=L/2$ is the value of x at which $u=1$ at $t=0$. This formula describes the way the slope of the u curve decreases with time. To understand the way the shock front propagates in Figs. 2 and 3 we need in addition the conservation theorem

$$\int_0^L u\,dx=\text{const} , \tag{2.3}$$

which is easily derived from Eq. (2.1) and the periodic boundary conditions. Applying this to the triangular regions of base $d=$ position of shock front and height $u(d)=d/(t+d_0)$ in Figs. 2 or 3 we find

$$\begin{gathered}\tfrac{1}{2}d_0=\tfrac{1}{2}d\frac{d}{t+d_0} ,\\ d=[d_0(t+d_0)]^{1/2} ,\end{gathered} \tag{2.4}$$

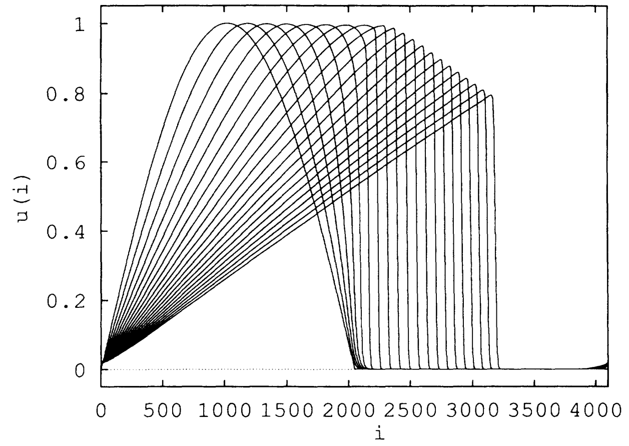

FIG. 3. Solution of the Burgers equation (2.1) at equally spaced time intervals for an initial condition $u(x,0)=\sin(2\pi x/L)$, $0\le x\le L/2$; $u(x,0)=0$, $L/2\le x\le L$. The x interval is represented on a grid of 4096 points, $x/L=i/4096$, $i=1,4096$. As time advances the curves steepen, developing a moving shocklike discontinuity. The time interval between curves is 160 in grid units, i.e., $\Delta t u_{\max}/a=160$ with $a=L/4096$ and $u_{\max}=1$. The calculation was performed with a finite-differencing scheme on a grid with 4096 points. In units of the grid spacing $\nu=2.048$, corresponding to a Reynolds number $4096/2.048=2000$.

$$u(d)=\left[\frac{d_0}{t+d_0}\right]^{1/2} . \tag{2.5}$$

The general appearance of the curves in Figs. 1–3 is thus easily explained. We are concerned here with how to obtain accurate numerical solutions of the nonlinear partial differential equation (2.1) in an efficient way. We hope that techniques found in the study of the Burgers equation will be useful in more difficult and interesting cases, such as the problems of fluid mechanics.

III. MATRIX ELEMENTS OF DIFFERENTIAL OPERATORS

Expanding $u(x,t)$ in any convenient orthonormal basis $\phi_i(x)$,

$$u(x,t)=\sum_{i=1}^{\infty} u_i(t)\phi_i(x) , \tag{3.1}$$

the Burgers equation (2.1) becomes

$$\frac{\partial u_i}{\partial t}=\nu a_{ij}u_j+b_{ijk}u_ju_k , \tag{3.2}$$

where

$$a_{ij}=\int dx\, \phi_i(x)\frac{\partial^2\phi_j(x)}{\partial x^2}$$

$$=-\int dx\frac{\partial\phi_i(x)}{\partial x}\frac{\partial\phi_j(x)}{\partial x} , \tag{3.3}$$

$$b_{ijk}=-\int dx\, \phi_i(x)\phi_j(x)\frac{\partial\phi_k(x)}{\partial x} . \tag{3.4}$$

Evaluation of these matrix elements for the Daubechies functions can be carried out analytically using the recursive and orthogonality properties of the scaling and wavelet functions. The general case for scaling functions all at the same level of resolution has been considered by Latto, Resnikoff, and Tenenbaum [12]. Here we review their results and show explicitly how to expand those results to include only a subset of the wavelets of various scales in the set of basis functions.

The problem of computing matrix elements such as a_{ij} and b_{ijk} can be divided into four stages. First, calculate the matrix elements for scaling functions which are translates of one another, all referring to the same level of resolution. Second, include the wavelet functions at that same level. Third, find the scaling law (usually a power of $\sqrt{2}$) to convert the previous results to other levels of resolution (i.e., all functions at a new but common level of resolution). Finally, evaluate the matrix elements for basis functions at differing levels of resolution. All four stages make use of the basic scaling relations for the functions

$$\phi_{n,i}(x)\equiv\frac{\phi_0\left[\dfrac{x}{2^n}-i\right]}{\sqrt{2^n}} , \tag{3.5}$$

$$\psi_{n,i}(x)\equiv\frac{\psi_0\left[\dfrac{x}{2^n}-i\right]}{(2^n)^{1/2}} , \tag{3.6}$$

where the fundamental scaling function ϕ_0 and associated wavelet function ψ_0 satisfy

$$\phi_0(x)=\sqrt{2}\sum_{j=0}^{N-1} c_j\phi_0(2x-j) , \tag{3.7}$$

$$\psi_0(x)=\sqrt{2}\sum_{j=0}^{N-1} c_{N-1-j}(-1)^j\phi_0(2x-j) , \tag{3.8}$$

and the c_j's are the Daubechies coefficients of order N.

We now illustrate the method on the simple first-derivative matrix elements

$$d_{ij}\equiv\int dx\, \phi_i(x)\frac{\partial\phi_j(x)}{\partial x} . \tag{3.9}$$

Start at the finest ($n=0$) level with $\phi_{0,i}(x)=\phi_0(x-i)$. Because, within this set of functions, the integral d_{ij} depends only on the difference of the indices, a single index suffices. Using the scaling relation (3.7) yields

$$d_j\equiv\int dx\, \phi_0(x)\frac{\partial\phi_0(x-j)}{\partial x}=2\sum_{k,l} c_lc_{l+k-2j}d_k . \tag{3.10}$$

These homogeneous equations for the d_j's are not independent and must be supplemented by additional equations including at least one inhomogeneous equation to set the scale for d_j. Such additional equations can be obtained from the moment conditions, which say that only the scaling functions $\phi_{0j}(x)$ are needed to represent exactly the functions 1, x, x^2, etc., up to an order which depends on which set of Daubechies functions is used. Again using scaling yields

$$1=\sum_i \phi_0(x-i)\ , \tag{3.11}$$

$$x=\sum_i (i+s_0)\phi_0(x-i)\ , \tag{3.12}$$

with $s_0 \equiv \sum_k k/\sqrt{2}$, from which results, by taking a derivative and substituting an expression for 1 inside an integral,

$$0=\sum_i d_i\ , \tag{3.13}$$

$$1=\sum_i i d_i\ . \tag{3.14}$$

Replacing any one of the homogeneous equations (3.10) (except $j=0$) with the inhomogeneous equation (3.14) yields a set of linear equations which can be solved for the d_j's.

For the matrix elements between ψ_0's the scaling relation (3.8) gives

$$d_j^{\psi}=2\sum_{k,l}(-1)^k c_l c_{l+k-2j} d_k = 4d_{2j}-d_j\ , \tag{3.15}$$

where use has been made of the relation

$$\sum_l c_l c_{l+2i}=\delta_{0,i}\ , \tag{3.16}$$

which follows from orthonormality of the ϕ_{0j}'s.

Mixed matrix elements d_j^m, with m standing for *mixed*, are found just as easily from

$$d_j^m \equiv \int dx\ \phi_0(x)\frac{\partial\psi_0(x-j)}{\partial x}$$
$$=2\sum_{k,l}(-1)^{k+l}c_l c_{N-1-k-l+2j} d_k\ . \tag{3.17}$$

This takes care of the matrix elements at the finest level of resolution. To obtain those at coarser levels, use is made of the fact that any ϕ or ψ at a coarse level of resolution is a linear combination of ϕ's at the next-finer level, as seen from the definitions Eqs. (3.5) and (3.6) using the scaling relations Eqs. (3.7) and (3.8), i.e.,

$$\phi_{n,i}(x)=\sum_j c_j \phi_{n-1,2i+j}(x)\ , \tag{3.18}$$

$$\psi_{n,i}(x)=\sum_j (-1)^j c_{N-1-j}\phi_{n-1,2i+j}(x)\ . \tag{3.19}$$

Thus the matrix elements at any level of resolution can be found from those at finer levels by carrying out the linear transformations of Eqs. (3.18) and (3.19) iteratively, directly on the matrix elements, beginning with the d_j's and d_j^m's we have just constructed. This transformation is called a discrete wavelet transform (DWT) (see Rioul and Duhamel [15] for a recent review; the specific implementation we used is that of Press [16]) and could be carried out in a straightforward way on the M $(=2^m)$ by M matrix we have just constructed in the ϕ_0,ψ_0 basis.

On the other hand, since we do not want to keep all the wavelets at all levels, but choose a subset at each level, we do not need to evaluate the full M by M matrix. We found it faster, therefore, to use the scaling properties of the ϕ's and ψ's to avoid redundant calculation. Each level of coarseness has functions which are twice as wide and $1/\sqrt{2}$ times as high and therefore have first-derivative matrix elements which are $\frac{1}{2}$ the size of those at the next-finer level. This takes care of all matrix elements between basis functions at equal levels. For the mixed-level elements we found an efficient method is to build up the desired matrix by adding one basis function at a time, starting with the scaling functions at the coarsest level and adding wavelet functions beginning at the largest scale and working down to finer scales. The required additional row and column can be computed from a DWT on the matrix of d_j^m's appropriate to the current level of ψ's and discarding any unneeded elements. To illustrate, let us assume we have a list of the wavelets we want to keep, and that we are adding the last wavelet and thus the last row and column, to be labeled by $(n,j)=(0,j_0)$, to our matrix. We take the vector

$$v_i \equiv d^m_{j_0-i}=\int dx\ \phi_0(x-i)\frac{\partial\psi_0(x-j_0)}{\partial x} \tag{3.20}$$

for $i=1$ to $M/2$ and perform a DWT on the index i. The resulting vector contains the desired matrix elements plus those between $\psi_0(x-j_0)$ and wavelets which we are not including in our list. The desired ones can be read out using our list. While some elements were thus calculated and then discarded, this method has the advantage that one never discards an entire row or column, as would be the case if a two-dimensional DWT were done on the full ϕ_0,ψ_0 matrix.

The calculation of the b_{ijk} elements is done similarly. In this case two supplementary equations are required in addition to the scaling equations. We used

$$1=\sum_j j b_{j,j,0}\ , \tag{3.21}$$

$$0=\sum_j b_{j,1+j,0}\ . \tag{3.22}$$

For the mixed-level elements, the situation is even more critical here than for the two-dimensional a_{ij} case. Here, successively adding functions to the basis requires adding shells to the array using small-size two-dimensional DWT's, which is much better than doing the full-size three-dimensional DWT.

IV. TIME STEPPING

Returning now to the Burgers equation (3.2) in any chosen basis, advancing in time can be done by several methods. We used a second-order semi-implicit time-stepping scheme which allows large time steps and provides good accuracy:

$$c_{ij}u_j^{n+1} \equiv \left[\delta_{ij}-\nu\frac{dt}{2}a_{ij}-\frac{dt}{2}(b_{ijk}+b_{ikj})u_k^n\right]u_j^{n+1}$$
$$=\left[\delta_{ij}+\nu\frac{dt}{2}a_{ij}\right]u_j^n\ . \tag{4.1}$$

Any complete orthogonal basis can be employed in the above equations. We want to use a set that will provide a good description of the developing discontinuity at the shock front without requiring a large number of states which are just wasted. With a uniformly distributed finite-differencing scheme, for example, a large number of points in the neighborhood of the discontinuity implies an unnecessarily high point density at other positions. Figure 3 was produced with a finite-differencing scheme employing 4096 equally spaced grid points, but obviously the high density of points is unnecessary except in the neighborhood of the discontinuity.

Expansion in a set of fine-scale scaling functions, as employed in Refs. [7,8,11], does not seem to change this aspect appreciably. Individual scaling functions are spread out over six neighboring grid sites when one uses Daubechies-6 basis states, but one still needs a very fine scale for the underlying grid in order to obtain a good description of the discontinuity and avoid the Gibbs-like oscillations which those authors found. This implies an unnecessarily high density of states centered about points away from the discontinuity.

We have used a basis consisting of a modest number N_s of coarse-scale scaling functions plus a selected set of wavelets of finer scales. We chose a fixed number N_w of wavelets centered about the discontinuity at each successive level of finer (by factors of 2) scaling out to some maximum. For example, Figs. 1 and 2 were produced using $N_s=32=2^5$ and $N_w=12$ out to a resolution level corresponding to a maximum of $N_{\max}=4096=2^{12}$ possible functions, i.e., $32+7\times 12=116$ scaling functions and wavelets. Thus we hoped to do almost as well with 116 suitably chosen scaling functions and wavelets as we would have done with the 4096 lowest-order scaling functions and wavelets.

The matrix c on the left-hand side of Eq. (4.1) must be inverted to carry out the time stepping. In a finite-differencing scheme the matrices a and b involve just nearest neighbors, the matrix c is tridiagonal, and the inversion is very fast. If one uses a basis of scaling functions, as recommended by Tenenbaum and co-workers, the computation of c is fast and c is a banded matrix (with four nonzero elements above and four below the main diagonal in a Daubechies-6 basis). The inversion of such a banded matrix is also fast. For a basis using both scaling functions and wavelets as discussed in the preceding paragraph, the matrix c is sparse, but with a rather complicated distribution of zeros. We found it necessary to use dense matrix programs to invert c. The most time-consuming part of the calculation turned out to be the evaluation of c, which requires computer time $\propto N^3$ with $N=N_s+7N_w=116$, the number of modes kept.

For the initial condition leading to Fig. 1 the discontinuity is fixed in time. For such a case one choice of the set of N_w wavelets to be kept is good for all time. If the singularity moves, as in Figs. 2 and 3, the set of N_w wavelets to be kept must change with time, i.e., the code must be adaptive. In general this would require recalculation of the matrices a and b for each time step and would probably be quite expensive. For the particular problem discussed in this paper we were able to evade this difficulty by exploiting the periodic boundary conditions. With this type of boundary condition all points are equivalent and the discontinuity can be shifted so as to always be at the center of the range. Thus after each time step we inverted the wavelet transform so as to get back to coordinate space, located the point on the curve of maximum negative slope, translated the curve so this point was at the center, and performed the forward wavelet transform so as to get back into wavelet space for the next time step, keeping track all the while of how far the curves had been translated in order to be able to construct the plots in coordinate space at successive times, as shown in Figs. 1 and 2.

V. RESULTS AND CONCLUSIONS

Our results using a selected set of $N_s=32$ coarse-scale scaling functions and $7\times N_w=84$ wavelets, for a total of 116 from the lowest 4096, are shown in Figs. 1 and 2 for the full-sine-wave and half-sine-wave initial conditions. For comparison, a finite-differencing calculation using 4096 equally spaced points for the half-wave initial condition is shown in Fig. 3. No finite-differencing calculation is shown for the full-sine-wave initial condition because it is indistinguishable from Fig. 1. It is clear from comparing Figs. 2 and 3 that 116 suitable chosen modes do almost, but not quite, as well as 4096 for the half-sine-wave initial condition.

Experimentation showed that $N_s=32$ is the minimum leading to acceptable results for the half-sine-wave initial condition, but that N_w can be reduced from 12 to 6 and $N_{\max}$ can be reduced from 4096 to 1024, i.e., $32+5\times 6=62$ modes, with a slight decrease in the quality of the result. Of course these reductions lead to a big savings in computer time.

The calculations given in our plots were made with a value of $\nu=2.048$ in grid units. Since the maximum value of u has been fixed at 1, this corresponds to a "Reynolds number" of $4096/2.048=2000$. We found by experimenting that ν could be reduced to 0.512, corresponding to a Reynolds number of 8000 without noticeably changing the results for the half-sine-wave initial condition. Further reduction in ν led to instabilities. For the full-sine-wave initial condition ν could be reduced even further. It is not, however, possible to go to the limit $\nu=0$.

In conclusion, we find that it is possible to obtain good results for the solution of the Burgers equation with initial conditions leading to shock waves by employing a small set of suitably selected coarse-scale scaling functions and fine-scale wavelets chosen to describe the behavior near the discontinuity. We are able to do almost as well with 116 scaling functions and wavelets as with 4096 uniformly spaced points. For this one-dimensional problem the added overhead of the wavelet computation is unfortunately more than the cost of a finite difference calculation with a large number of equally spaced points. We might hope that for a higher-dimensional problem the reward would be greater than the cost.

ACKNOWLEDGMENTS

This work was supported by the Physics Department and the Campus Research Board of the University of Illinois at Urbana-Champaign.

[1] Ingrid Daubechies, *Ten Lectures on Wavelets*, CBMS-NSF Regional Conference Series in Applied Mathematics Vol. 61 (SIAM, Philadelphia, 1992).

[2] Marie Farge, Annu. Rev. Fluid Mech. **24**, 395 (1992).

[3] IEEE Trans. Inf. Theory **38**, 529 (1992) (special issue on wavelets).

[4] Gilbert Strang, SIAM Rev. **31**, 614 (1989).

[5] G. Beylkin, R. Coifman, and V. Roklin, Commun. Pure Appl. Math. **44**, 141 (1991).

[6] S. Mallat, IEEE. Trans. Pattern Anal. Mach. Intell. **PAMI-11**, 674 (1989); Trans. Am. Math. Soc. **315**, 69 (1989).

[7] John Weiss, Aware, Inc. Report No. AD910628.1, 1991 (unpublished).

[8] A. Latto and E. Tenenbaum, C. R. Acad. Sci. Ser. I **311**, 903 (1990).

[9] Y. Maday, V. Perrier, and J.-C. Ravel, C. R. Acad. Sci. Ser. I **312**, 405 (1991).

[10] R. Glowinski, W. Lawton, M. Ravachol, and E. Tenenbaum, in *Wavelet Solutions of Linear and Nonlinear Elliptic, Parabolic and Hyperbolic Problems in One Space Dimension*, Proceedings of the 9th International Conference on Numerical Methods in Applied Sciences and Engineering (SIAM, Philadelphia, 1990), pp. 55–120.

[11] Aware, Inc. Report No. AD900615.2, 1990 (unpublished).

[12] A. Latto, H. L. Resnikoff, and E. Tenenbaum, Aware, Inc. Report No. AD910708, 1991 (unpublished).

[13] G. B. Whitham, *Linear and Nonlinear Waves* (Wiley, New York, 1974), Chap. 4.

[14] S. N. Gurbatov, A. N. Malakhov, and A. I. Saichev, *Nonlinear Random Waves and Turbulence in Nondispersive Media: Waves, Rays and Particles* (Manchester University Press, Manchester, 1991).

[15] O. Rioul and P. Duhamel, IEEE Trans. Inf. Theory **38**, 569 (1992).

[16] W. H. Press, Harvard-Smithsonian Center for Astrophysics Report No. 3184, 1991 (unpublished).